Available online at www.sciencedirect.com
SCIENCE DIRECT
Journal of Photochemistry and Photobiology A: Chemistry 181 (2006) 314–324
Journal of Photochemistry and Photobiology A:Chemistry
www.elsevier.com/locate/jphotochem

Photocatalytic and photochemical degradation of mono-, di- and tri-azo dyes in aqueous solution under UV irradiation

Cláudia Gomes Silva, Wendong Wang [1], Joaquim Luís Faria *

Laboratório de Catálise e Materiais, Departamento de Engenharia Química, Faculdade de Engenharia da Universidade do Porto, Rua Dr. Roberto Frias s/n, 4200-465 Porto, Portugal

Received 15 September 2005; received in revised form 13 December 2005; accepted 14 December 2005
Available online 23 January 2006

Abstract

The degradation of three commercially available textile azo dyes, Solophenyl Green BLE 155% (SG), Erionyl Red B (ER) and Chromotrope 2R (C2R), has been studied by using photochemical and photocatalytic processes under UV irradiation. The adequacy of each process depends on the concentration of dye. At low dye concentration, the neat photochemical degradation is very efficient. The photocatalytic process, using either slurry of Degussa P-25 TiO_2 or a biphasic mixture of TiO_2 and activated carbon (AC), more effectively bleaches heavier colored solutions. The heterogeneous photocatalytic regime was characterized in terms of catalyst load, TiO_2 to AC mass ratio, initial dye concentration and oxygen partial pressure. Catalyst recovery and reuse was also analyzed. Based on the Langmuir–Hinshelwood approach, reaction rates and adsorption equilibrium constants were calculated. A positive effect on the photocatalytic degradation was observed by the addition of AC to TiO_2 catalyst, which was quantified in terms of a synergy factor (R). The efficiencies of different photo-induced degradation processes were compared based on the experimentally determined apparent rate constants, mineralization degrees and initial quantum yields.

Keywords: Photochemistry; Photocatalysis; Titanium dioxide; Activated carbon; Azo dyes

1. Introduction

In spite of the current trend to find more selective and efficient chemical processes, there is still a current need for treating used waters, especially in the industries where is an intensive consumption, such as textile and printing. Industrial dyestuffs including textile dyes are recognized as being an important environmental threaten. In nowadays more than half of the dyes available on the market are azo compounds, which can be grouped as monoazo, diazo, triazo according to the number of azo bonds (−N=N−) in its structure. Their widespread use makes them as one of principal sources of contamination of used waters. Adequate treatment of these waters is of primary concern in order to preserve the natural ecosystem. The biological processes are more natural and easy to implement but they have a major drawback, which is the production of sludge proportionally to the volume of treated water. When the volume to treat is huge, recycling is essential.

Nevertheless, used water always requires some treatment prior to reuse, with or without addition of fresh water. The extent of the treatment depends either on the degree of contamination, or on the requirements of the next use. Chemical treatments provide adequate response to a number of specific cases, because with them the pollutant is not being transferred, rather converted, or in the ideal case mineralized.

New developments in advanced oxidation processes (AOPs) are attractive in providing a promising and competitive solution for the abatement of numerous hazardous compounds in wastewater including Fenton or photo-assisted Fenton process, ozone or/and peroxide photolysis, and semiconductor photocatalysis process [1–6]. AOPs feature the capability of utilizing the high reactivity of hydroxyl radicals to drive oxidation processes, which are suitable for achieving the complete elimination and full mineralization of various pollutants, such as phenols [7], chlorophenols [8], pesticides [9] and azo dyes [10].

* Corresponding author. Tel.: +351 225 081 645; fax: +351 225 081 449.
E-mail address: jlfaria@fe.up.pt (J.L. Faria).
[1] Present address: Department of Materials Science and Engineering, University of Science and Technology of China, Hefei 230026, PR China.

1010-6030/$ – see front matter © 2005 Elsevier B.V. All rights reserved.
doi:10.1016/j.jphotochem.2005.12.013

In this sense, due to fast development of light related technologies, the photochemical processes are positioning themselves on a privileged position to compete with other available technologies. Photocatalytic degradation (PCD) processes, assisted by a semiconductor metal oxide (normally as photocatalyst) and oxygen (as primary oxidizing agent), earn increasing importance in the area of wastewater treatment as the most emerging destructive technology [1–11]. Contributing to this are the facts that these processes require mild operation conditions of temperature and pressure and in many cases result in total mineralization of the pollutants without any waste disposal problem. Water treatment processes based on heterogeneous photocatalysis, principally concerning TiO_2-assisted photocatalytic degradation of azo dyes, have been reviewed recently [10,12,13]. The most extensively used photocatalyst is TiO_2 and the TiO_2/UV system has been widely investigated in PCD processes. According to the usually proposed mechanism, irradiation of TiO_2 particles with suitable photons energy ($h\nu \geq E_g = 3.25$ eV) generates a bound electron/hole pair which can dissociate in competition with recombination to produce a conduction band electron (e_{cb}^-) and a valence band hole (h_{vb}^+). Both charge carriers scan the TiO_2 surface to reduce adsorbed electron acceptors and oxidize adsorbed electron donors. For PCD processes in aqueous system, oxygen is often present as the electron acceptor to form superoxide anion radical ($O_2^{\bullet -}$), while H_2O and OH^- are available as electron donors to yield hydroxyl radical ($HO^\bullet$). Both of the radicals are very reactive and strongly oxidizing, capable of totally mineralizing most of the organic compounds.

The photocatalytic activity of TiO_2 largely depends on its microstructure and physical properties [14–16] as well as on incorporation of some other metal ions, adsorbents or supports [17–19]. It has been reported that carbon materials have some beneficial effects on the photocatalytic activity of TiO_2 by inducing synergies or cooperative effects between the metal oxide and carbon phases [20–26]. To incorporate carbon with TiO_2 particles different preparation methods are currently in use. One of the simplest and somewhat successful approaches results from mechanically mixing TiO_2 with activated carbon (AC). Although not the most effective, it has the advantage of being easy to implement, therefore suitable for small to medium size textile and dying plants. In the present work, three textile commercial azo dyes, Solophenyl Green BLE 155% (SG), Erionyl Red B (ER) and Chromotrope 2R (C2R), which correspond to tri-, di- and mono-azo dyes, have been chosen as the target substrates. The photodegradation of these dyes over TiO_2 photocatalyst and TiO_2 and activated carbon mixture under UV light was studied in detail as well as the photolysis processes.

2. Experimental

2.1. Materials

Degussa P-25 titanium dioxide (Degussa Portuguesa) was used as photocatalyst. The material consists mostly of the anatase form, with a BET surface area of 55 $m^2\,g^{-1}$ and a mean particle size of 30 nm (manufacturer data).

Solophenyl Green BLE 155% and Erionyl Red B are commercially available from Ciba-Geigy (Ciba Portuguesa Lda). Dye Chromotrope 2R is a standard from Fluka (27410, 2-(phenylazo)chromotropic acid disodium salt). The dyes were used as received without any further purification. In Table 1 is given the Color Index classification of each dye, as well as some physical–chemical characteristics of the three azo dyes. Their structures are drawn in Fig. 1. Molecular weights are given by the supplier, while spectroscopic data was determined experimentally.

Granular activated carbon NORIT C-GRAN (NORIT Nederland B.V.) consists in a high adsorptive capacity material, produced by chemical activation using the phosphoric acid process, which possesses a very open porosity (macro- and meso-pore) and a BET surface area of 1400 $m^2\,g^{-1}$ (supplier data). In order to facilitate suspension the grains were ground in a mortar and sieved. The mean diameter of the resulting particles ranged from 0.1 to 0.3 mm.

2.2. Photoreactor and photodegradation experiments

We performed the photolytic and photocatalytic tests using an immersion glass reactor of 1000 ml, charged with 800 ml of solution/suspension. The UV irradiation source located axially and held in a quartz immersion tube consisted of a low-pressure mercury vapor lamp Heraeus TNN 15/32 with a dominant emission line at 253.7 nm (3 W of radiant flux). The photoreactor was kept inside an opaque box to protect the operator from exposure to UV radiation and avoid interference of the artificial external light. A magnetic bar stirred the reaction mixture and a typical experiment was carried out in open-air conditions. Nevertheless, the reactor was equipped with a gas feeding system capable of providing different partial pressures of oxygen to the solution/suspension.

In the photochemical degradation experiments, we used an initial concentration between 5 and 50 $mg\,l^{-1}$ in all aqueous solutions of the dyes. In a typical experiment, we dissolved the calculated amount of dye in the desired volume of distilled water immediately before the beginning of the reaction. Samples (ca. 5 ml) were regularly withdrawn at controlled times and immediately analyzed by UV–vis spectroscopy.

Table 1
Characteristics of the studied azo dyes

Name	Dye class	Azo type	M_w (g/mol)	λ_{max} (nm)	ε_{max} ($M^{-1}\,cm^{-1}$)
Solophenyl Green BLE 155% (C.I. Direct Green 26)	Direct	Triazo	1338	610	27560
Erionyl Red B (C.I. Acid Red 151)	Acid	Diazo	478.46	550	10000
Chromotrope 2R (C.I. Acid Red 29)	Acid	Monoazo	468.39	509	24147

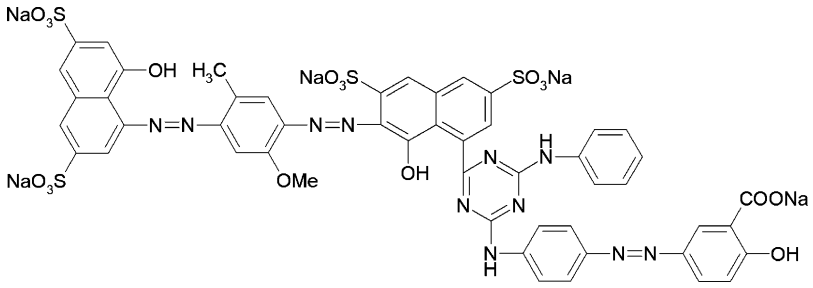

Solophenyl Green BLE 155% (SG)

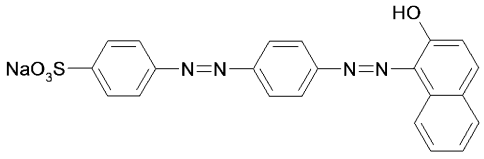

Erionyl Red B (ER)

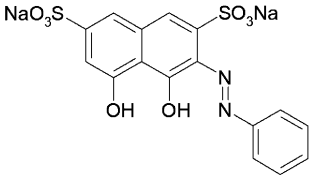

Chromotrop 2R (C2R)

Fig. 1. Chemical structures of the azo dyes: triazo Solophenyl Green BLE 155%, diazo Erionyl Red B and monoazo Chromotrope 2R.

We established the optimal amount of TiO_2 for the photocatalytic degradation, using SG as probe molecule, fixing its initial concentration before the dark adsorption period (details follow) to 50 mg l^{-1} and varying the amount of titania from 50 to 2000 mg l^{-1}.

In the experiments involving the biphasic catalyst, the activated carbon was ground and then added into the TiO_2 suspension. For the kinetic studies, we varied independently the initial concentration of dye and the TiO_2/AC ratios.

In a typical photocatalytic experiment, the suspension containing the dye was stirred in the dark for 30 min allowing the adsorption–desorption quasi-equilibrium to be established. We chose this lapse of time, based on the results of preliminary experiments where we found that more than 75% of the maximum adsorption capacity of the TiO_2 reached almost instantaneously and kept constant for approximately 1 h. We determined the adsorption isotherms for each dye after an adsorption period of 24 h at room temperature and found the following maximum adsorption capacities: 40.69 mg_{dye}/g_{TiO_2} for SG, 11.54 mg_{dye}/g_{TiO_2} for ER and 1.586 mg_{dye}/g_{TiO_2} for C2R.

One first sample was taken out for analysis at the end of the dark adsorption period, just before turning on the illumination, in order to determine the bulk dye concentration. This value was taken as the initial concentration for the photocatalytic experiment, denoted hereafter as C_0 (in addition to C_0', the initial bulk concentration of dye before dark adsorption). Samples were regularly withdrawn from the reactor, centrifuged immediately for separation of the suspended solids, and the clean transparent solution analyzed by UV–vis spectroscopy.

2.3. UV–vis spectroscopic analysis

The full spectrum (250–750 nm) of each sample was recorded on a JASCO V-560 UV–vis spectrophotometer (double monochromator and double beam optical system) and the absorbance at selected wavelengths registered. For kinetic analysis, each sample taken from the reactor was divided into three different vials and the final absorption was given by the arithmetic average over the three measurements. Since the λ_{max} (Table 1) of the dyes is well in the medium to long wavelength range, dye concentration can be directly evaluated from this

absorbance. However, during the degradation experiments the full spectra was carefully analyzed in order to avoid interference of any non-colored by-products.

The UV–vis reflectance spectra of the solid materials were recorded on the same JASCO spectrophotometer equipped with an integrating sphere attachment (JASCO ISV-469). The powders were not diluted in any matrix to avoid a decrease of the absorbance. The instrument software converted the diffuse reflectance spectra to equivalent absorption Kubelka–Munk units [27]. These units express the peak intensity measure calculated from the reflectance of a diluted sample of infinite depth upon application of the Kubelka–Munk mathematical function.

2.4. Determination of pH of point of zero charge (pH_{pzc})

The pH_{pzc} was determined using the mass titration method described elsewhere [28]. Following the usual protocol a set of 0.01 M $NaNO_3$ solutions at pH 3, 6 and 11 was prepared from 0.1 M HNO_3 and 0.1 M NaOH solutions. For each starting pH an increasing amounts of TiO_2 (0.1, 0.5, 1, 2.5, 5 and 10%, w/w) were added to 50 ml of the $NaNO_3$ solutions. The equilibrium pH was measured after 24 h of shaking at room temperature (approximately 20 °C).

2.5. Photocatalysts recovery and reutilization

In the experiments where TiO_2 was used alone as photocatalyst, after finishing the reaction, the suspension was filtered to recover the solid, which was rinsed with water and dried at 110 °C for 24 h. The recovered photocatalyst was then ground and washed again with a mixture of distilled water and ethanol to remove any trace of adsorbed compounds. At the end of this operation, TiO_2 was again dried and ground before reuse in the photocatalytic reaction.

2.6. TOC analysis

In order to determine the degree of mineralization total organic carbon (TOC) measurements were performed using a Shimadzu 5000-A TOC analyzer. Samples consisting of 10 ml aliquots were taken when complete color removal was observed. This could occur at different times depending on the dye and operating conditions. If necessary, samples were centrifuged prior to analysis.

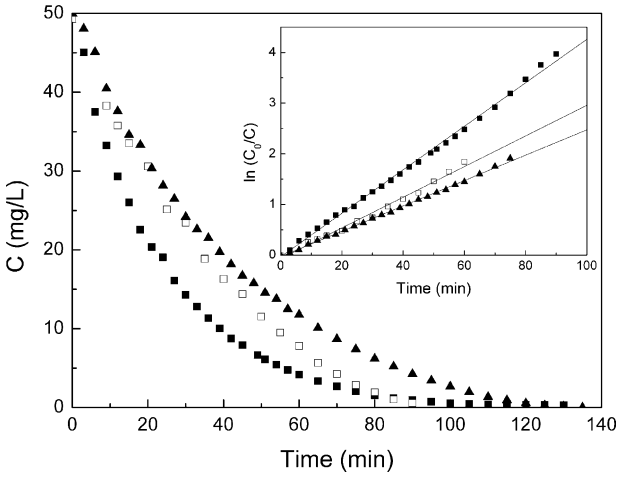

Fig. 2. Kinetics of degradation of azo dyes in aqueous solutions during photochemical degradation with an initial concentration (C_0) of 50 mg l^{-1}: (■) SG; (□) ER; (▲) C2R (inset: linear transform of $\ln(C_0/C)$ vs. t).

3. Results and discussion

3.1. Photolytic degradation under UV irradiation

As we demonstrated in a recent work [26], direct photolysis of azo dyes under UV light cannot be ignored in this process. UV radiation alone bleaches colored aqueous solutions by destruction of the chromophore group ($R_1-N{=}N-R_2$) of the dye [10].

Following the variation on the absorption spectra of the dye aqueous solutions during the photochemical reaction, we could observe that the dye concentration decreases exponentially with time, disappearing after some minutes, resulting in complete decolorization of the solutions (Fig. 2). The observed exponential decay can be described in terms of a pseudo-first-order kinetic model:

$$-\frac{dC}{dt} = k_{UV}C \quad (1)$$

where k_{UV} is the pseudo-first-order kinetic constant and C is the concentration of dye. Integration of Eq. (1) results in a linear dependency of $\ln(C_0/C)$ on t with a slope of k_{UV} (Fig. 2, inset). It can be seen that even for concentrated solutions (50 mg l^{-1}), the reaction time is very fast, which make this a very feasible process.

The initial concentration of dye was varied from 5 to 50 mg l^{-1} and the effect on the conversion and decolorization

Table 2
Apparent first-order rate constants (k_{UV}) and conversion at 9 min after turning on UV illumination (X_9) during photochemical degradation for different initial dye concentration

C_0 (mg l^{-1})	k_{UV} (min^{-1})			X_9 (%)		
	SG	ER	C2R	SG	ER	C2R
50	0.042 ± 0.001	0.030 ± 0.001	0.024 ± 0.001	33	22	19
30	0.068 ± 0.001	0.057 ± 0.003	0.044 ± 0.001	48	33	29
20	0.086 ± 0.001	0.076 ± 0.003	0.066 ± 0.001	57	41	44
10	0.180 ± 0.005	0.19 ± 0.01	0.136 ± 0.007	83	77	67
5	0.270 ± 0.008	0.28 ± 0.03	0.23 ± 0.02	91	99	90

rate of the three azo dyes is shown in Table 2. There is an obvious correlation between the kinetic rate constants k_{UV} and the initial concentration of dye C_0: higher the dye concentration, lower the value of k_{UV}. A 10-fold increase in the initial concentration of the dyes leads to a 6-fold decrease in the rate constant of the process in the case of the SG dye and a 9-fold decrease for the two other dyes, ER and C2R. An inner filter effect caused by the less availability of photons as the color of the solution gets more intense can explain these observations.

It is also noticeable from Table 2 that a significant conversion of the dyes can be obtained after short irradiation times, confirming the high efficiency of this process of color removal. For lighter colored solutions (initial dye concentration of 5 mg l^{-1}), it is possible to reach almost total decolorization within 9 min of reaction time.

3.2. Photocatalytic degradation over TiO_2

The photocatalytic degradation of azo dyes under UV light in the presence of TiO_2 also follows the pseudo-first-order kinetics with respect to the dye concentration:

$$-\frac{dC}{dt} = k_{app}C \quad (2)$$

where k_{app} is the apparent first-order constant. Integration results in a linear dependency of $\ln(C_0/C)$ on t with a slope of k_{app}, which will be used to evaluate the activities of the catalysts under different conditions in the following investigation.

3.2.1. Effect of catalyst loading

The optimal amount of titania to achieve the maximum efficiency of the photocatalytic process depends on the nature of the photocatalyst, the geometry of the reactor, the incident radiant flux and the mean optical pathway within the suspension [29]. The catalyst dosage as an important parameter has been extensively studied in many photocatalytic reactions [30], suggesting that the optimal TiO_2 dosage varies from 0.15 to 2.5 g l^{-1}. In the present study, we used the SG dye as model and followed its photocatalytic degradation to determine the optimal concentration of catalyst.

As shown in Table 3, when TiO_2 concentration varied from 0.050 to 2.000 g l^{-1} at a constant initial concentration of SG dye before dark adsorption of 50 mg l^{-1}, k_{app} increased with the mass of TiO_2 up to an amount of 1 g l^{-1}. This indicates a true heterogeneous catalytic regime. The observed increase in the apparent rate constant with the concentration of titania till this optimal value probably results from an increment of the active sites available for adsorption and degradation of the dye. Higher quantity of catalyst in the suspension, leads to lower initial concentration values of dye after dark adsorption (C_0), which confirms an enhancement of adsorption capacity of dye on the catalyst and therefore results in higher apparent rate constants. On the other hand, the decrease in the apparent rate constant with TiO_2 concentration higher than 1 g l^{-1} probably results from a screening effect due to the redundant dispersion of UV radiation caused by suspended photocatalyst, masking part of the photosensitive surface. Additionally, in the case of heavy loads we observed agglomeration and sedimentation of TiO_2 making a significant fraction of the catalyst to be inaccessible to either adsorbing the dye or absorbing the radiation [31,32], with consequent decrease in the active sites available to the catalytic reaction.

Following these observations, we decided to keep the amount of TiO_2 at the optimum value of 1 g l^{-1} in subsequent photocatalytic degradation experiments for all dyes. The ratio TiO_2/AC was then arranged as function of this rule.

Table 3
Apparent first-order kinetic rate constants (k_{app}) for the photocatalytic degradation over TiO_2 with the same initial concentration of SG (50 mg l^{-1}) before dark adsorption period (C_0') and different concentrations of TiO_2 (C_{TiO_2})

C_{TiO_2} (mg l^{-1})	C_0' (mg l^{-1})	C_0 (mg l^{-1})	k_{app} (min^{-1})
50	50	47	0.026
100	50	45	0.029
250	50	40	0.032
500	50	32	0.034
1000	50	20	0.047
2000	50	17	0.044

3.2.2. Effect of different dyes adsorption properties

It is noticed that the three azo dyes display different adsorption behaviors over TiO_2 during dark adsorption period, which is expected due to their different chemical structures. For the triazo dye SG, the initial dye concentration after the dark adsorption period decreased to 20 mg l^{-1} (Table 3), while this value decreases by 8 and 3 mg l^{-1} for the diazo dye ER and the monoazo dye C2R, respectively. In all cases the amount of dye exceeds the maximum adsorption capacity provided by the TiO_2 (see Section 2.2). The observed decrease in dye concentration can be explained in terms of different electrostatic interactions between the various dyes and the catalyst surface, which depends on the pH value of the dye solutions. This dependence could be considered as the intrinsic amphoteric behavior of the catalyst and the acidic nature of the dye [33], which can be described by the following chemical equilibrium equations:

$$TiOH + H^+ \leftrightarrows TiOH_2^+ \quad (3)$$

$$TiOH + OH^- \leftrightarrows TiO^- + H_2O \quad (4)$$

Therefore, it is reasonable to consider that the dye adsorption process on the photocatalyst surface depends on the electrical charge of both dye and catalyst.

The pH of the point of zero charge (pH_{pzc}) for the TiO_2 Degussa P-25 used in the photocatalytic experiments was determined by mass titration at different initial pH from the asymptotic value reached by the pH as the mass fraction of titania increases (Fig. 3). The value of pH_{pzc} is 6.0, which is in agreement with the results reported previously [34,35]. When pH values of aqueous dye solution is lower than TiO_2 pH_{pzc}, the catalyst surface develops a positive charge and attractive forces between catalyst and dye can promote the adsorption process. Increasing the pH of dye solution, leads to the situation where the electrostatic charge on the TiO_2 surface will become less positive, or even negative if the point of zero charge is surpassed,

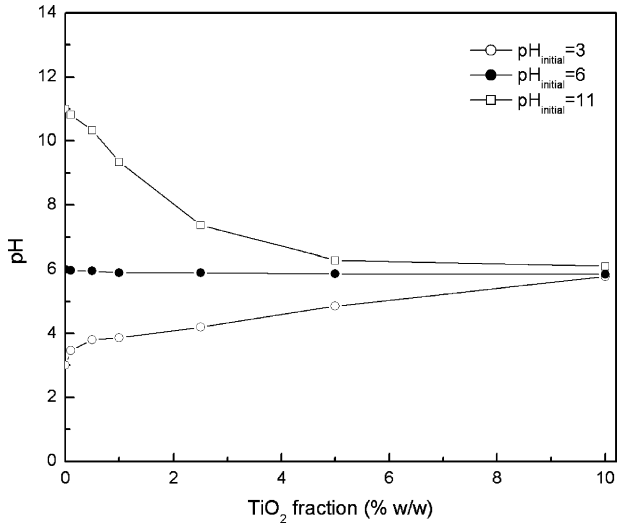

Fig. 3. Determination of pH_{pzc} of TiO_2 Degussa P-25. Results of mass titration at initial pH of 3 (◯), 6 (●) and 11 (□).

developing repulsive forces between the catalyst and the dye, therefore decreasing dye adsorption [31–33].

There are negatively charged sulphonic groups (SO_3^-) in the chemical structure of all the studied dyes, and all the reactions were performed in their natural pH conditions without any pH adjustment. In the case of SG dye, the pH value of aqueous suspensions was 5.6 approximately lower than TiO_2 pH_{pzc}, which result in the most intense adsorption on TiO_2 surface. The suspensions containing ER and C2R dyes showed pH values of 5.8 and 5.9, respectively, higher than the pH of SG suspensions and more approximated to TiO_2 pH_{pzc}, which may account for the smaller quantity of both dyes adsorbed on TiO_2 surface during the dark adsorption period.

3.2.3. Effect of oxygen partial pressure

The presence of an electron acceptor is essential to enhance the separation of photo-generated electrons and holes, improving the efficiency of the photocatalytic process. Oxygen dissolved in the solution is commonly employed as the electron acceptor.

We conducted a detailed study on the effect of oxygen partial pressure for the photocatalytic degradation of SG dye under UV irradiation over TiO_2. The oxygen partial pressure was adjusted by diluting it in helium, and maintaining the overall flow rate at $10\,ml\,s^{-1}$ for a total gas pressure at 1 atm. The initial dye concentration (C_0') was kept at $50\,mg\,l^{-1}$ and the concentration of TiO_2 at $1\,g\,l^{-1}$. The comparison parameter was the reaction rate constant.

As shown in Fig. 4, the first-order rate constant increased with the oxygen partial pressure. The rate constant reached about 85% of its maximum value at an oxygen partial pressure of 0.3 atm. This fact indicates that it is feasible to operate under ambient air condition instead of pure oxygen for commercial application purpose. This was in fact the case for the further kinetic studies in the present work.

Following a first-order Langmuir–Hinshelwood kinetic model, the effect of oxygen partial pressure on the degradation

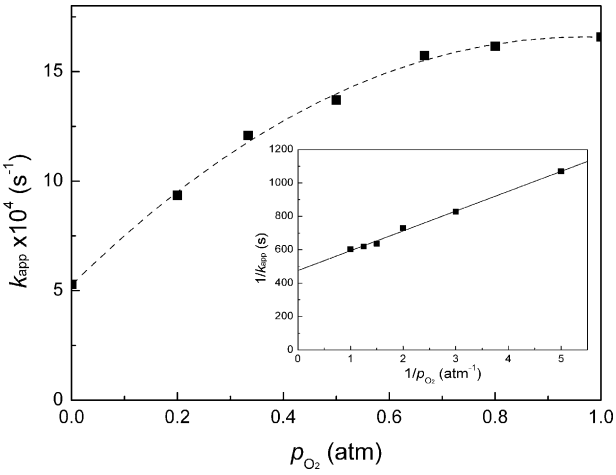

Fig. 4. Effect of oxygen partial pressure on the photocatalytic degradation rate of SG dye over TiO_2 under UV irradiation.

kinetic rate constant (k_{app}) can be described as

$$r = k_r \frac{K_{ads}}{1 + K_{ads} C_0} \frac{K_{O_2} p_{O_2}}{1 + K_{O_2} p_{O_2}} C \tag{5}$$

which can be rearranged in

$$r = k_1 \frac{K_{O_2} p_{O_2}}{1 + K_{O_2} p_{O_2}} C = k_{app} C \tag{6}$$

where p_{O_2} is the oxygen partial pressure, K_{O_2} the adsorption constant of dissolved oxygen on TiO_2 surface and k_1 is an adjustable parameter, which includes the rate constant k_r and depends on the experimental conditions. A simple transformation will give a linear relationship between $1/k_{app}$ and $1/p_{O_2}$ as

$$\frac{1}{k_{app}} = \frac{1}{k_1 K_{O_2}} \frac{1}{p_{O_2}} + \frac{1}{k_1} \tag{7}$$

The value of K_{O_2} obtained from the linear regression (Fig. 4, inset) in this study is $4.01\,atm^{-1}$, which is comparable to that reported in literature [30].

3.2.4. Determination of adsorption equilibrium constant K_{ads} and reaction rate constant k_r

The results of photocatalytic degradation of SG, ER and C2R under UV irradiation over TiO_2 are summarized in Table 4 as function of the initial dye concentration ranges, after dark adsorption. It is observed that the apparent rate constant values (k_{app}) decreases as the dye concentration increases, which may be explained in terms of the increasing difficulty of UV radiation to penetrate into the aqueous suspensions. Higher the initial concentration of the dye, fewer the photons reaching the catalyst surface, lesser the photo-efficiency of the process.

Similar to the previous section, the kinetics of the photocatalytic degradation are well described by a modified Langmuir–Hinshelwood model. Considering that the amount of oxygen dissolved in the suspension is constant and that the adsorption coefficients of all organic molecules present in the reacting mixture are effectively equal, the equation for a first-

Table 4
Apparent first-order rate constants (k_{app}) and conversion at 9 min after turning on illumination (X_9) during photocatalytic degradation over TiO_2 with different initial concentrations of dyes (C_0)

C_0 (mg l^{-1})	k_{app} (min^{-1})			X_9 (%)		
	SG	ER	C2R	SG	ER	C2R
41–50	0.024 ± 0.001	0.059 ± 0.001	0.023 ± 0.001	13	48	23
31–40	0.039 ± 0.001	0.073 ± 0.002	0.028 ± 0.001	30	52	28
21–30	0.047 ± 0.001	0.102 ± 0.003	0.037 ± 0.001	34	66	31
11–20	0.072 ± 0.002	0.169 ± 0.009	0.048 ± 0.001	52	83	37
5–10	0.078 ± 0.002	0.230 ± 0.008	0.083 ± 0.003	57	87	45

order kinetic reaction follows:

$$r = \frac{k_r K_{ads}}{1 + K_{ads} C_0} C = k_{app} C \quad (8)$$

in which k_r and K_{ads} are the kinetic rate constant and the adsorption equilibrium constant, respectively. Thus the linear relationship between $1/k_{app}$ and C_0 can be expressed as

$$\frac{1}{k_{app}} = \frac{C_0}{k_r} + \frac{1}{k_r K_{ads}} \quad (9)$$

Following Eq. (9), the values for reaction rate constant k_r and adsorption equilibrium constant K_{ads} can be determined by linear regression from the plot of $1/k_{app}$ and C_0 (Table 5). These values will be used in the following sections to evaluate the enhancement obtained when the activated carbon is introduced in the system.

3.2.5. Catalyst recovery and reuse

Catalyst deactivation is one of the drawbacks on the application of TiO_2 to photocatalytic degradation of organic pollutants, due to the strong adsorption of the original compound and/or by-products on the active sites of the catalyst surface [24,36,37]. The color change of the used catalyst after photocatalytic degradation reactions may indicate the effects of chemisorption and chemisorbed species reconstruction processes on the degradation mechanism. These occurrences can be investigated from the UV–vis diffuse reflectance spectra of initial TiO_2 and used catalyst after photocatalytic degradation of SG, ER and C2R dyes (Fig. 5).

As expected, TiO_2 has no bands above its fundamental absorption sharp edge rising at 400 nm. Enhancement of the absorption is visible for the used catalysts, decreasing in order of SG, ER and C2R, probably correlated to the number of azo bonds in their chemical structure.

The recovered catalysts were reused in another resumed photocatalytic experiment with fresh aqueous solution of the corresponding dye, and the results are compared in Table 6. It is observed that the rate constants decrease in all cases by about 30%. This decline of the kinetics is ascribed to the presence of adsorbed species on the active sites of the catalyst surface and on the change of the dimension of the catalyst particles. The later may result from the recovery procedure (described in Section 2.5). Both factors account for the reduction of the number of available photoactive sites.

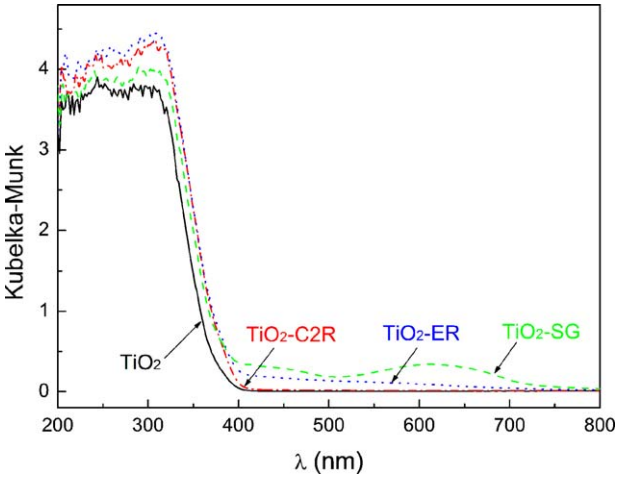

Fig. 5. Diffuse reflectance absorption spectra of fresh TiO_2 P-25 and recovered TiO_2 (TiO_2-dye) after being used in photocatalytic degradation of SG, ER and C2R.

3.3. Photocatalytic degradation over TiO_2 and activated carbon mixture

3.3.1. Effect of activated carbon loading

The optimal amount of activated carbon was determined using the SG dye as reference system. Based on the optimized reaction conditions indicated in the previous sections, the con-

Table 5
Reaction rate constants (k_r) and adsorption equilibrium constants (K_{ads}) for photocatalytic degradation over TiO_2 by the modified Langmuir–Hinshelwood model

Dye	k_r (mg l^{-1} min^{-1})	K_{ads} (mg^{-1} l)
SG	1.58	0.092
ER	2.43	0.143
C2R	1.26	0.128

Table 6
Apparent first-order rate constants (k_{app}) during photocatalytic degradation over fresh (k^1_{app}) and recovered (k^2_{app}) TiO_2 for different dyes with the initial dye concentration $C_0 \approx 50$ mg l^{-1}

Dye	k^1_{app} (min^{-1})	k^2_{app} (min^{-1})
SG	0.024 ± 0.001	0.018 ± 0.001
ER	0.059 ± 0.001	0.040 ± 0.001
C2R	0.023 ± 0.001	0.015 ± 0.001

Table 7
Apparent first-order rate constants (k_{app}) and SG concentration after 30 min of dark adsorption (C_0) for the photocatalytic degradation over TiO_2 + AC at different AC loads (C_{AC})

C'_0 (mg l^{-1})	C_0 (mg l^{-1})	C_{AC} (mg l^{-1})	k_{app} (min^{-1})
50	20	0	0.047 ± 0.001
50	26	50	0.048 ± 0.001
50	33	100	0.052 ± 0.002
50	38	200	0.055 ± 0.001
50	40	300	0.053 ± 0.001

centration of TiO_2 in the suspension was kept at 1 g l^{-1} and the initial concentration (C'_0) of SG dye at 50 mg l^{-1}, while the concentration of AC was varied from 0 to 300 mg l^{-1}. The effect of the AC load on the apparent first-order rate constants of photodegradation is described in Table 7.

From the data given in Table 7, it is clear that the photocatalytic degradation of SG dye over TiO_2 + AC mixture is more efficient than that over TiO_2 alone (Table 4). The highest value of k_{app} is obtained for AC content of 200 mg l^{-1}, which corresponds to an optimal weight ratio of AC to TiO_2 at 1/5. For a higher AC concentration, the decrease in efficiency of the photocatalytic process can be attributed to an excessive content of activated carbon particles contacting directly with TiO_2 surface, therefore reducing the number of photoactive sites.

We observed that the amount of SG adsorbed during the dark period decreases as the AC content of the TiO_2 + AC mixture increases, showing that the TiO_2 + AC mixture exhibits a lower adsorption capacity than TiO_2 alone. The same decrease in adsorption capacity was observed in case of the other dyes, ER and C2R. The explanation for this observation may lie on the creation of an interface between TiO_2 and AC, where the AC is covered by the excess TiO_2, therefore not being able to act as co-adsorbent and at the same time limiting the number of sites accessible to the adsorption of dye molecules [20,38].

3.3.2. Synergy in photocatalytic degradation of azo dyes over TiO_2 + AC mixture

The results on the photocatalytic degradation of SG, ER and C2R under UV irradiation over TiO_2 + AC mixture are summarized in Table 8. When k_{app} is used as comparing parameter, it is clear that the overall efficiency of the photocatalytic process over TiO_2 + AC mixture is significantly higher than that over TiO_2, in varying degrees (see Table 4). This suggests an effect

Table 8
Apparent first-order rate constants (k_{app}) and synergy factors (R) for photocatalytic degradation processes over TiO_2 + AC mixture with different initial concentrations of dyes

C_0 (mg l^{-1})	k_{app} (min^{-1})			R		
	SG	ER	C2R	SG	ER	C2R
41–50	0.048	0.063	0.034	2.00	1.07	1.48
31–40	0.055	0.078	0.044	1.41	1.07	1.57
21–30	0.065	0.096	0.051	1.38	–	1.38
11–20	0.094	0.113	0.074	1.31	–	1.54
5–10	0.120	0.180	0.133	1.54	–	1.60

Table 9
Reaction rate constants (k_r) and adsorption equilibrium constants (K_{ads}) for photocatalytic degradation over TiO_2 + AC mixture determined by the modified Langmuir–Hinshelwood model

Dye	k_r (mg l^{-1} min^{-1})	K_{ads} (mg^{-1} l)
SG	2.64	0.0928
ER	4.22	0.0558
C2R	1.70	0.1966

like synergy of activated carbon in TiO_2 + AC mixture for the photocatalytic degradation of azo dyes.

It is possible, and a synergy factor R has been suggested previously [20,26] to quantify the extent of this effect for the photocatalytic process over TiO_2 + AC in relation to TiO_2 alone. It is defined in terms of the apparent rate constants, as follows:

$$R = \frac{k_{app}(TiO_2 + AC)}{k_{app}(TiO_2)} \quad (10)$$

The synergy factors calculated for each azo dye are listed in Table 8. In case of the higher colored suspension ranged at 41–50 mg l^{-1}, the highest value of synergy factor R of 2.00 is obtained for SG dye, which means a double k_{app} value when AC was introduced into the TiO_2 suspension in this case. For ER and C2R dyes, the values are 1.07 and 1.48, respectively. In the case of ER there is a less pronounced effect which is expectable since this dye was already very efficiently removed in the neat photochemical process.

Following Eq. (9), the values of the reaction rate constant k_r and the adsorption equilibrium constant K_{ads} can be determined by linear regression from the plot of $1/k_{app}$ versus C_0 using the data from Table 8. The obtained values are listed in Table 9.

Compared to the results over TiO_2 alone (Table 5), it is unambiguous that the reaction rate constants (k_r) increased remarkably for all the three azo dyes, suggesting that the presence of AC plays an important role in the reaction kinetics of the photocatalytic degradation process.

However, the effect of AC on the adsorption equilibrium constants (K_{ads}) is quite random with respect to different dyes. If it is assumed that the AC will be mainly covered by the TiO_2 in excess, the adsorption abilities should not be changed, except for the fact that the number of adsorption sites will be reduced. However the interphase interaction is somehow relevant in the case of the adsorption of the small molecules. For the heavier tri-azo dye SG, the values of K_{ads} are comparable, but those for ER and C2R are different and not correlated. These results indicated that AC accounts for the adsorption of the degradation process depending on the type of pollutants. As mentioned earlier, solutions of ER ad C2R exhibit higher pH values than that of SG; and the activated carbon used in the photocatalytic experiments possesses slightly acid surface, therefore this difference in K_{ads} values could be attributable to the electrostatic interaction of the azo dyes molecules and the surface of the activated carbon.

Additionally, since TiO_2 and AC are just mechanically mixed, there is no fine control on the interphase formation between them. To circumvent this disadvantage, TiO_2 and carbon com-

posite catalyst can be synthesized using a sol–gel procedure [25] prior to the introduction into the reaction solution.

3.4. Comparison of different photo-induced degradation processes of azo dyes

Based on the results presented above concerning photocatalytic degradation over TiO_2 + AC mixture, TiO_2 alone and neat photolytic degradation of a series of azo dyes, we compared the efficiency of the different photo-induced degradation processes in terms of their apparent rate constants, mineralization and quantum yields. For application purposes, the same initial concentration before dark adsorption at 50 mg l^{-1} is used, which is close to the concentrations found in some stream waters of textile processes.

3.4.1. Evaluation on apparent rate constants

A global comparison based on the apparent first-order rate constants, between the three photo-induced degradation processes for the studied azo dyes is pictured in Fig. 6. The photocatalytic processes appear to be more efficient than the neat photolysis. The results demonstrate an obvious advantage in the photocatalytic process using a suspension with TiO_2 + AC mixture instead of TiO_2 alone, featuring the synergy caused by the introduction of AC. The extent of this effect varies for the different azo dyes, and it is more evident in the case of the ER.

3.4.2. Evaluation on mineralization

The TOC removal is a practical way to evaluate the efficiency of a degradation process, from an application point of view. Since the measurements were performed at full decolorization of the suspension, the results reflect the actual degree of the mineralization of the organic pollutants rather than the reaction kinetics of the photolytic and photocatalytic degradation processes.

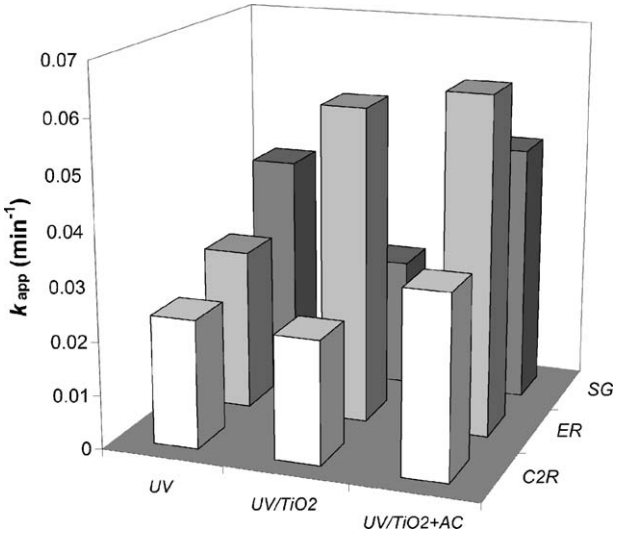

Fig. 6. Comparison of the apparent first-order rate constants for the different photo-induced degradation processes of azo dyes solutions.

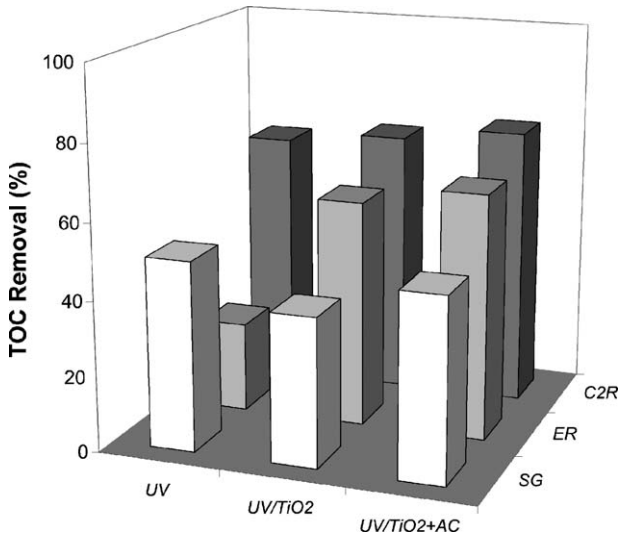

Fig. 7. Comparison of TOC removal for the different photo-induced degradation processes of azo dyes solutions.

Fig. 7 reaffirms the advantage of photocatalytic process with comparison to the neat photolysis, which again is more obvious for the degradation of ER dye. On the other hand, the introduction of AC does not affect mineralization in the same magnitude as observed for reaction rates. The overall mineralization degree is at maximum 75%, indicating that there is still a residual amount of organic compounds, consisting of low weight molecules such as aldehydes and carboxylic acids [39], in the treated solution. Unfortunately some of these by-products may be even more toxic than the original compounds [40]. A possible way to remove these undesirable by-products is to extend the irradiation time in order to achieve the complete mineralization of the organics.

3.4.3. Evaluation on quantum yield

From the point of view of energy consumption, it is important to evaluate the photonic efficiency of the process. By definition, the quantum yield (Φ) of a particular photophysical or photochemical process is the number of molecules which react according to this process divided by the number of photons absorbed by the system during the same time [41]. From a kinetic standpoint, the initial quantum yield can be defined as the ratio of the reaction rate (r_0) in molecule per second to the efficient photonic flux (φ) in Einstein per second [3] according to

$$\Phi_0 = \frac{r_0}{\varphi} \tag{11}$$

The value of the quantum yield may vary on a wide range, according to the characteristic of catalysts, the experimental conditions and especially the nature of reactions under consideration.

The photonic flux (φ) is related to the radiant power of the lamp used in the degradation experiments as well as the wavelength of radiation emission. In the present work, a low-pressure mercury lamp was used with an emission line at 253.7 nm providing 3 W of radiant flux. Considering an efficient radiant power of 75%, the efficient photonic flux was equal to

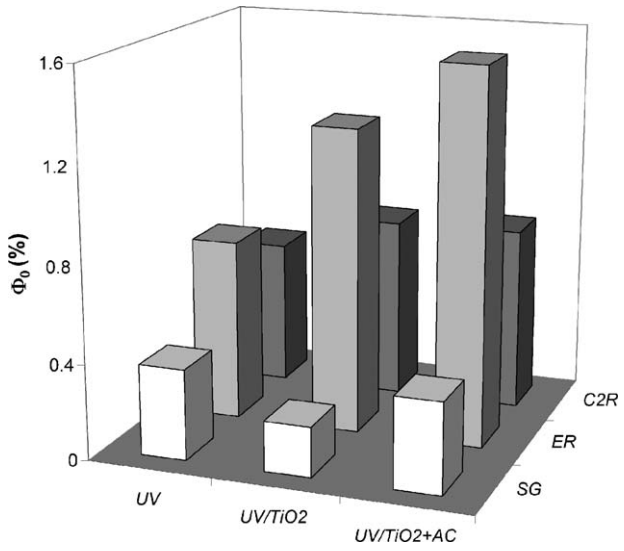

Fig. 8. Comparison of the initial quantum yields for the different photo-induced degradation processes of azo dyes solutions.

2.87×10^{18} photons s^{-1}. The initial quantum yields (Φ_0) estimated for the different photo-induced degradation processes of the azo dyes are compared in Fig. 8.

Consistent with the evaluation on the rate constant and TOC removal, these results favor the benefit of the photocatalytic processes and the introduction of AC, which features higher photo efficiency during the photocatalytic processes especially for the degradation of ER dyes. These conclusions also agree well with the previous studies on photodegradation of organic pollutants [29,42,43].

4. Conclusions

Direct photolysis of aqueous solutions of the dyes Chromotrope 2R, Erionyl Red B and Solophenyl Green BLE 155%, under UV light at the wavelength of 253.7 nm revealed to be an efficient process for decolorizing the solution, provided the initial concentration of dye is low. The degradation of heavily colored solutions can be achieved more effectively by means of the photocatalytic processes over TiO_2 alone and TiO_2 + AC mixture. The apparent rate constants generally varied in an inverse relation to the initial concentration of the dyes in the solutions. This can be attributed to an inner filter effect for the pure photochemical process and a screening effect in the case of the photocatalytic process, where the excess of dye blocks the photosensitive surface of the catalyst reducing the availability of photoactive sites.

The photocatalytic reaction conditions were optimized concerning the catalyst loading, oxygen partial pressure and the amount of activated carbon in TiO_2 + AC mixture. The optimum concentration of TiO_2 was 1 g l^{-1} and the optimum ratio of AC to TiO_2 was 1/5 for TiO_2 + AC mixture. The presence of oxygen did not provide any effect on the kinetics of the photochemical process, while the rate constants increased with the partial pressure of oxygen in the suspensions in the case of the photocatalytic processes. The reutilization of the recovered TiO_2 resulted in a slightly decrease in the efficiency varied for the photocatalytic degradation of different azo dyes.

A positive effect on the efficiency parameters was observed on the photocatalytic degradation over TiO_2 + AC mixture when compared to TiO_2 alone, which was explained in terms of a synergy induced by the introduction of AC. Following a modified Langmuir–Hinshelwood model, the reaction rate constant and adsorption equilibrium constant were determined. The increase in reaction rate constant is real for all the three dyes over TiO_2 + AC mixture with comparison to TiO_2 alone.

The efficiency of the different photo-induced degradation processes was evaluated in terms of apparent rate constants, mineralization degrees and initial quantum yields. Overall, the results revealed the superiority of photocatalytic processes over neat photolysis and the advantage of using a suspension of TiO_2 + AC mixture instead of TiO_2 alone.

It was not possible to establish a direct relationship between the structure characteristic of the azo dyes (for example the number of azo bonds) and the kinetics of the photo-induced degradation processes. The decomposition of this type of organic compounds depends on several factors including their acidic nature, affinity to the catalyst surface, functional groups in molecular structure, etc.

From a standpoint of a real case application, the results showed that the photo-induced degradation processes proved to be efficient for solutions of dyes currently used in textile industries. The process is rather simple and requires very inexpensive catalysts, but energy consumption has to be taken into account. In case of real textile wastewaters, due to the high complexity of its composition, a combination of physical and chemical treatments may be required to achieve the desired levels of water bleaching. The degree of treatment will depend on the final destination of the used waters: reuse or discharge.

Acknowledgements

Thanks are given to Dr. R.A. Boaventura (LSRE/FEUP) for the sample of Solophenyl Green BLE 155% dye (a gift from Ciba Portuguesa Lda) and for the permission to use some of its laboratory facilities; to NORIT Nederland B.V. for the activated carbon; to Degussa Portuguesa for TiO_2 P-25. This research was carried out under the projects POCTI/33401/EQU/2000, POCI/EQU/58252/2004, POCTI/1181/2003, SFRH/BD/16966/2004 and SFRH/BPD/11598/2002, approved by the Fundação para a Ciência e a Tecnologia (FCT), Programa Operacional (POCTI and POCI) and co-supported by FEDER.

References

[1] O. Legrini, E. Oliveros, A.M. Braun, Chem. Rev. 93 (1993) 671–698.
[2] R. Andreozzi, V. Caprio, A. Insola, R. Marotta, Catal. Today 53 (1999) 51–59.
[3] J.M. Herrmann, Catal. Today 53 (1999) 115–129.
[4] K. Pirkanniemi, M. Sillanpaa, Chemosphere 48 (2002) 1047–1060.
[5] S. Malato, J. Blanco, A. Vidal, C. Richter, Appl. Catal. B 37 (2002) 1–15.
[6] P.R. Gogate, A.B. Pandit, Adv. Environ. Res. 8 (2004) 501–551.

[7] J. Sykora, M. Pado, M. Tatarko, M. Izakovic, J. Photochem. Photobiol. A 110 (1997) 167–175.
[8] M. Pera-Titus, V. Garcia-Molina, M.A. Banos, J. Gimenez, S. Esplugas, Appl. Catal. B 47 (2004) 219.
[9] I.K. Konstantinou, T.A. Albanis, Appl. Catal. B 42 (2003) 319–335.
[10] I.K. Konstantinou, T.A. Albanis, Appl. Catal. B 49 (2004) 1–14.
[11] D.S. Bhatkhande, V.G. Pangarkar, A. Beenackers, J. Chem. Technol. Biotechnol. 77 (2002) 102–116.
[12] J.M. Herrmann, Top. Catal. 34 (2005) 49–65.
[13] D.F. Ollis, Top. Catal. 35 (2005) 217–223.
[14] P.S. Awati, S.V. Awate, P.P. Shah, V. Ramaswamy, Catal. Commun. 4 (2003) 393–400.
[15] G. Sivalingam, K. Nagaveni, M.S. Hegde, G. Madras, Appl. Catal. B 45 (2003) 23–28.
[16] M. Toyoda, Y. Nanbu, Y. Nakazawa, M. Hirano, M. Inagaki, Appl. Catal. B 49 (2004) 227–232.
[17] M. Anpo, M. Takeuchi, J. Catal. 216 (2003) 505–516.
[18] S. Anandan, M. Yoon, J. Photochem. Photobiol. C 4 (2003) 5–18.
[19] E.P. Reddy, L. Davydov, P. Smirniotis, Appl. Catal. B 42 (2003) 1–11.
[20] J. Matos, J. Laine, J.-M. Herrmann, Appl. Catal. B 18 (1998) 281–291.
[21] J. Arana, J.M. Dona-Rodriguez, E.T. Rendon, C.G.I. Cabo, O. Gonzalez-Diaz, J.A. Herrera-Melian, J. Perez-Pena, G. Colon, J.A. Navio, Appl. Catal. B 44 (2003) 153–160.
[22] B. Tryba, A.W. Morawski, M. Inagaki, Appl. Catal. B 41 (2003) 427–433.
[23] S. Qourzal, A. Assabbane, Y. Ait-Ichou, J. Photochem. Photobiol. A 163 (2004) 317–321.
[24] J. Arana, J.A.H. Melian, J.M.D. Rodriguez, O.G. Diaz, A. Viera, J.P. Pena, P.M.M. Sosa, V.E. Jimenez, Catal. Today 76 (2002) 279–289.
[25] W.D. Wang, P. Serp, P. Kalck, J.L. Faria, Appl. Catal. B 56 (2005) 305–312.
[26] C.G. da Silva, J.L. Faria, J. Photochem. Photobiol. A 155 (2003) 133–143.
[27] J.W. Niemantsverdiet, Spectroscopy in Catalysis, VCH, Weinheim, 1995.
[28] H. Valdes, M. Sanchez-Polo, J. Rivera-Utrilla, C.A. Zaror, Langmuir 18 (2002) 2111–2116.
[29] A. Assabane, Y.A. Ichou, H. Tahiri, C. Guillard, J.M. Herrmann, Appl. Catal. B 24 (2000) 71–87.
[30] D.W. Chen, A.K. Ray, Appl. Catal. B 23 (1999) 143–157.
[31] C.M. So, M.Y. Cheng, J.C. Yu, P.K. Wong, Chemosphere 46 (2002) 905–912.
[32] T. Sauer, G.C. Neto, H.J. Jose, R. Moreira, J. Photochem. Photobiol. A 149 (2002) 147–154.
[33] F. Kiriakidou, D.I. Kondarides, X.E. Verykios, Catal. Today 54 (1999) 119–130.
[34] Y.X. Chen, K. Wang, L.P. Lou, J. Photochem. Photobiol. A 163 (2004) 281–287.
[35] J. Fernandez, J. Kiwi, J. Baeza, J. Freer, C. Lizama, H.D. Mansilla, Appl. Catal. B 48 (2004) 205–211.
[36] J. Arana, E.T. Rendon, J.M.D. Rodriguez, J.A.H. Melian, O.G. Diaz, J.P. Pena, Appl. Catal. B 30 (2001) 1–10.
[37] L.X. Cao, Z. Gao, S.L. Suib, T.N. Obee, S.O. Hay, J.D. Freihaut, J. Catal. 196 (2000) 253–261.
[38] J. Matos, J. Laine, J.-M. Herrmann, J. Catal. 200 (2001) 10–20.
[39] R.L. Cisneros, A.G. Espinoza, M.I. Litter, Chemosphere 48 (2002) 393–399.
[40] H.M. Pinheiro, E. Touraud, O. Thomas, Dyes Pigment 61 (2004) 121–139.
[41] A.M. Braun, M.-T. Maurette, E. Oliveros, Photochemical Technology, John Wiley & Sons Ltd., Chichester, England, 1991.
[42] M. Vautier, C. Guillard, J.M. Herrmann, J. Catal. 201 (2001) 46–59.
[43] D.W. Chen, A.K. Ray, Water Res. 32 (1998) 3223–3234.